JOURNAL OF SCIENCE TECHNOLOGY AND EDUCATION 9(3), SEPTEMBER, 2021
ISSN: 2277-0011; Journal homepage: www.atbuftejoste.com

Effects of Variance of Pore Size Distribution on Mercury Entrapment

Nuradeen Tanko
Department of Petroleum and Gas Engineering,
Baze University, Abuja-FCT, Nigeria.

ABSTRACT
In literature, corrugated pore structure model (CPSM) simulation and random pore bond network in various research has established a significant finding in the transport relationship of porous media. These findings have shown a direct correlation that shows an increase in mercury entrapment as the variance of the pore size distribution gets wider. However, there is no experimental work on porous materials to support these significant findings. In this regard, this work attempted to verify the effect of Pore-size distributions on entrapment by an experimental approach. The materials studied are chemically pure mesoporous silica and alumina catalyst support pellets with simplified pore sizes, pore size distribution, and surface chemistry. The pore size distribution of the samples was obtained from the physical adsorption of the nitrogen Barrett-Joyner-Halenda algorithm. The entrapment of the samples was obtained from the retraction curves of mercury porosimetry. Therefore, a statistically significant correlation exists, and thus verifies the CPSM that mercury entrapment increases with an increase in the variance of the pore size distribution of the materials studied.

ARTICLE INFO
Article History
Received: June, 2021
Received in revised form: July, 2021
Accepted: August, 2021
Published online: September, 2021

KEYWORDS
Porous Media, Porosimetry, Pore Size Distribution, Mercury Entrapment

INTRODUCTION

In recent decades, Mercury porosimetry (MP) has been used by various researchers to identify those aspects of pore systems that affect the trapping of non-wetting fluids such as mercury, or by analogy oil and gas, in strongly water-wet systems (Meyer, 1953; Wardlaw & McKellar, 1981; Tsakiroglou, & Payatakes, 1990). Entrapment of mercury is recognized from the observation that, after the intrusion-extrusion cycle, the retraction curve does not give zero volume (Allen, 1991). The size, shape, and arrangement of conducting spaces in porous materials, such as reservoir rocks, are known to affect the flow of fluids and the displacement of one fluid by another (Tsakiroglou, 1990).

One of the earliest studies aimed at explaining the origin of hysteresis and entrapment was conducted with the aid of a two-dimensional network model consisting of cylindrical pore segments assembled into square grids (Androutsopoulost & Mann, 1978). These workers found that entrapment increased as the pore size distribution got wider and that mercury was preferentially entrapped in larger pores. Thus, this finding suggests that mercury retraction might involve a slower relaxation process as well as the more rapid, capillary flow process described by WASHBURN (2000). The workers attributed this slow retraction process to the formation of ganglia of entrapped mercury that, under a non-zero net force before equilibration, tends to move around slowly and may coalesce with the bulk. Therefore, it might be inaccurate to interpret mercury retraction solely based on a piston-like withdrawal.

In a similar approach, Wardlaw & McKellar (1981) built on the work of Androutsopoulost and Mann (1978) by conducting mercury porosimetry experiments (MPE) on model porous media consisting of various types of pore networks etched in the glass. The MPE, conducted by these researchers suggested that non-random structural heterogeneity causes mercury entrapment. It was found that, for mercury experiments on micromodels consisting of grids of pore elements of uniform size, no mercury entrapment occurred. Furthermore, no mercury entrapment occurred in glass micromodels where the sizes of individual, neighbouring pore grid elements were slightly different. Subsequently, a three-dimensional pore bond network modelling was adopted by Portsmouth (1991) to investigate the effects of the pore size distribution (PSD) and pore connectivity from the results of MPE. The inherent flexibility of this model facilitated the construction of networks with varying connectivities or distributions of

Corresponding author: Nuradeen, T. ✉ *nuradeen.tanko@bazeuniversity.edu.ng* ✉ *Department of Petroleum and Gas Engineering, Baze University, Abuja, FCT, Nigeria.*

connectivities. The results from simulations of standard intrusion/extrusion cycle porosimetry experiments suggested that there was a characteristic entrapment of mercury for a network comprising a Gaussian pore size distribution. Furthermore, the researchers stated that entrapment is dependent on the variance, $\frac{\sigma}{\mu}$, where σ is the standard deviation of the pore size distribution and μ is the mean pore size distribution.

In a different approach, Ioannidis and Chatzis (1993) expanded the concept of mixed-percolation on cubic lattices, representing pore bodies connected through pore throats, in a simulation to describe the phenomena of capillary pressure hysteresis and mercury entrapment. These researchers, model represented the pore structure of actual porous media in a 3-D regular cubic network consisting of pore bodies interconnected with pore throats. The pore bodies were modelled as cubes and pore throats as prisms. The key findings were that the pore size distribution, pore throat cross-sectional shape, and contact angle were found to be very significant in determining the retraction and the magnitude of mercury entrapment; and consequently, the magnitude of mercury retention. This finding is in good agreement with the work of Conner, Lane, and Hoffman (1984). However, Ioannidis and Chatzis (1993) assumption of pore bodies and throats as cubes and prisms are not generally compatible with all porous media even though it could be accepted for slit-shaped pores such as sandstones and dolomites (Tsakiroglou, 1990).

Mercury porosimetry (MP) is probably still the only method by which a macroscopic porous material can be characterised using just a single technique. In principle, MP can be used to obtain the porosity, specific pore volume, pore connectivity (Portsmouth, 1991), and the spatial distribution of pore size (Rigby, 2000; Rigby & Chigada, 2009). Gas adsorption and MP are complementary methods with the latter covering a much wider size range (0.0035 to 500 μm). There are well-known and standard techniques from gas sorption that can determine key characteristic parameters of porous media, such as the BET surface area (Brunauer, Emmett, & Teller, 1938), BJH algorithm for pore size distribution (Barrett, Joyner, & Halenda, 1951), and pore connectivity by percolation analysis (Liu & Seaton, 1994). Though it is sometimes possible to view pores with an electron microscope and to thereby obtain a measure of their diameter, it is difficult to measure the distribution of sizes, and impossible to representatively measure the associated surface area, particularly for a large sample. Therefore, these two complementary methods are still relevant in porosimetry.

In recent years, the wetting effects in the capillary condensation region have been studied extensively by Monte Carlo and MFDFT simulation (Nguyen, Do, & Nicholson, 2011; Rasmussen, Gor, & Neimark, 2012). These simulations suggested that the determination of distributions of pore characteristic dimension (typically diameter) are complicated by other pore geometrical properties, like length, and chemical properties, like adsorbate wetting, and experimental methods to assess these effects would be beneficial to improve the accuracy of pore size distributions. Hitchcock et al (2014) provided a complementary, definitive experimental study of integrated gas sorption and MP technique on disordered porous solids (silica or alumina). The integrated gas sorption and MP technique consist of running a series of gas sorption and MPE on the same sample by freezing any entrapped mercury in place before a subsequent gas sorption experiment. It was found that the wrong choice of adsorbate can lead to pore size inaccuracies of at least ~200% in characterizing silica-supported platinum catalysts. These results highlight particular issues for the accuracy of PSDs for catalysts consisting of metal nanoparticles supported on oxide materials. Similar observations were made earlier by Bafarawa et al. (2014) where they used integrated gas sorption, MP technique and mercury thermoporometry.

In a review, the micromodel experiments conducted by Wardlaw and McKellar (1981), and the network model of Androutsopoulost & Mann (1978) still offer good explanations of the entrapment of mercury after retraction. However, both share similar limitations, where they failed to verify their findings by conducting mercury experiments on porous media. It is in this regard that this paper further elucidates and expands the works of Wardlaw & McKellar (1981) and Androutsopoulost & Mann (1978). Emphasis is made on the retraction curve of MP, which is a source of useful information concerning mercury entrapment. The pore size distribution (PSD) is a widely used descriptor for the void space structure of disordered porous solids. Gas sorption is a very

Corresponding author: Nuradeen, T. ✉ nuradeen.tanko@bazeuniversity.edu.ng ✉ Department of Petroleum and Gas Engineering, Baze University, Abuja, FCT, Nigeria.

common experimental technique used to obtain the PSD, and thus will be adopted in this paper.

THEORY

The Mercury entrapment of mercury is recognized from the observation that, after the intrusion-extrusion cycle, the retraction curve does not give zero volume (Rigby et al., 2011) MP is based on the capillary rise phenomenon whereby an excess pressure is required to cause a non-wetting fluid (mercury) to climb up a narrow capillary (Lowell & Shields, 1981). The surface tension of mercury makes it difficult for it to enter small openings. Therefore, external pressure is required to overcome this opposition and force the mercury into the void spaces of the material (Allen, 1999). MP assessment of porous media covers mesoporosity (4 – 50 nm) and macroporosity (> 50 nm diameter). For the reasons stated above, MP has become the most favourite technique of characterizing void spaces in porous media (Orr, 1969). The conventional method of analyzing the resultant data from a porosimetry experiment relies on the use of a parallel pore bundle model originally introduced by WASHBURN, (2000). The Laplace equation, also known as the Washburn equation, can be employed to relate an applied pressure with a relevant pore diameter being intruded by the non-wetting liquid mercury.

$$\Delta p = \gamma_{HG}\left(\frac{1}{r_1}+\frac{1}{r_2}\right)=\frac{2\gamma_{HG}\cos\theta}{r_P} \quad 1.0)$$

The Washburn equation (Equation 1.0) relates the pressure difference across the curved mercury interface (r_1 and r_2 being the radii of curvature of that interface) to the corresponding pore size (r_p) using the surface tension of mercury (γ_{HG}) and the contact angle (θ) between the solid and mercury. The volume of mercury penetrating the pores is measured directly as a function of the applied pressure. According to Lowell & Shields (1981), a value of 0.485 N/m at 25 ˚C is generally accepted for surface tension and a fixed value of 130° for the contact angle (irrespective of the sample material). However, the surface or interfacial tension of mercury contributes greatly concerning errors in the determination of the pore size distribution and can change with a pore size (Lowell & Shields, 1981).

In addition, the Washburn equation (Equation 1.0) assumes the contact angle value of mercury and the cylindrical pore shape. However, various observations made by electron microscopy have shown that many traditional porous materials such as the silicas and aluminas appear to be random collections of packed spherical and hemispherical particles, as well as a cylinder (Giesche, 2006). Similar observations were seen in cement-based materials where the pore size is randomly distributed and most pores are connected to the surface of the sample through a chain of pores with varying sizes and shapes. Therefore, with such a pore structure, mercury cannot intrude into larger pores until the applied pressure is sufficient to force mercury to go through smaller throats.

Consequently, the standard MP results in an underestimate of large pores because of its intrinsic limitation due to ink-bottle type pores. These are pores that are connected to the surface by smaller neck entrances only, and thus, larger pores that are only accessible by smaller neck entrances will be underestimated in size and lead to hysteresis effects. The volume of these larger pores (ink-bottle pores) that is counted as the volume of smaller throats (pores) is referred to as the accessibility effect (Drewry & Seaton, 1995). Therefore, the Washburn Equation (1.0) constitutes a special model that fails to take into account that real the real nature of pores media consists of a network of interconnected circular pores. Such a model may not represent the pores in actual materials but it's generally accepted as the practical means of dealing with complex pore structures.

Despite the limitations addressed above, MP is widely used in the characterization of catalyst support pellets (Diamond, 2000; Rigby, Fletcher, & Riley, 2003), cement-based materials (Abell, Willis, & Lange, 1999; Ghaly, Beurroies, & Ragai, 2009), granite and saprolite materials (Stefan et al., 2006; Ma, 2014), and sedimentary rocks (Tsakiroglou and Payatakes, 1990; Moro & Böhni, 2002). In addition, the measured pore size distribution curves are frequently inclined towards small pore sizes, and thus MP cannot be used to analyse closed pores. Thus, the technique can only provide a valid estimate of pore structure, when the sample has pores directly accessible to mercury or that are easily reached by mercury through larger pores (Sing, 1985). Therefore, in this study, the PSD will be determined with the aid of Gas adsorption.

Adsorption pore size distribution analysis of mesoporous materials is based on an adopted interpretation of the mechanisms of capillary condensation, evaporation and the associated

Corresponding author: Nuradeen, T. ✉ *nuradeen.tanko@bazeuniversity.edu.ng* ✉ *Department of Petroleum and Gas Engineering, Baze University, Abuja, FCT, Nigeria.*

hysteresis phenomena (Seaton, Walton, & Quirke, 1989). The theory for condensation of vapour into a porous medium is derived from thermodynamic considerations. This is known as the Kelvin equation written as:

$$RT \ln x = \frac{-2\gamma_{LV} V_L \cos(\theta)}{r_K} \qquad (2.0)$$

Where r_K is the Kelvin radius. For nitrogen at liquid nitrogen temperature:

- γ_{LV} is the surface tension of the adsorbate in liquid form = 8.85 × 10^{-3} N m^{-2};
- V_L = 34.6 × 10^{-6} m^3 mol^{-1};
- R is the universal gas constant= 8.314 J mol^{-1} K^{-1};
- T is the temperature = 77 K;
- θ is the contact angle between the liquid and the wall of the pore = 0°.

Within a porous material, the gas layers continue to fill the pore until the pressure is sufficient that the gas condenses into a 'liquid-like phase'. The pressure at which the gas condenses can be related to the pore size according to the Kelvin equation. However, it becomes less accurate as the PSD becomes smaller because the Kelvin equation (Equation 2.0) is purely thermodynamic, and thus, it does not take account at micropore region (Lastoskie, Gubbins, & Quirke, 1993; Rouquerol, Llewellyn, & Rouquerol, 2007). This model has usually applied for diameters greater than 2nm because below this size the liquid cannot be considered a fluid with bulk properties due to forces exerted by the pore wall. Theoretical calculations suggest that the properties of fluids in microporous structures are highly sensitive to the size of the pores (Horvath, G. and Kawazoe, 1983).

In the case of mesopores, the Kelvin equation (Equation 2.0) provides a useful model for the transformation of adsorption data into a PSD (Lastoskie et al., 1993). There are established algorithms based on the Kelvin equation (Equation 2.0) that are used for the determination of PSD such as the Barrett Joyner and Halenda (BJH) method (Barrett et al., 1951). However, other approaches consider the fluid-solid interactions (Evbuomwan, 2009). The Horvath-Kawazoe (HK) method (Rouquerol et al., 2007), is a novel technique for determining the micropore size distribution. The method was originally used to analyse nitrogen adsorption on molecular sieve carbons with slit-shaped pores but has since been modified to account for cylindrical shaped pores as in the case of silica mesopores. The HK method is based on the general idea that the relative pressure required for the filling of micropores of a given shape and size, is directly related to the adsorbent - adsorbate interaction energy.

When the BJH algorithm is used to determine the PSD, the pore size obtained from the Kelvin equation is generally corrected for the multi-layer film thickness using a universal t -layer equation. The empirical observation by Rigby et al. (2011) has shown that, for many non-porous surfaces, the ratio of the volume adsorbed to the monolayer capacity $\left(\frac{V}{Vm}\right)$ plotted against relative pressure $\left(\frac{P}{P_0}\right)$ all approximately fit a common Type II curve above a relative pressure of 0.3. This implies for a given value of $\left(\frac{V}{Vm}\right)$ the adsorbed layer thickness will be the same regardless of the adsorbent. However, the data used to compile common t -curves were not comprehensive and the universality was only approximated Rigby et al. (2008). Therefore, an individual porous solid may show a deviation from the common *t*-curves, as observed experimentally for nonporous templated silicas, such as the SBA-15 using neutron scattering Schreiber et al. (2006).

In reality, the contact angle changes as the pore fill and the pore shape varies (Gregg, 1982). Therefore, for a wide distribution of pore sizes, and possibly, quite separately developed pore systems, a mean size is not sufficient. For an ink-bottle type pore, the pressure required to fill a neck with a cylindrical meniscus exceeds the pressure required to fill a body via a hemispherical meniscus, with a neck radius that exceeds 0.5 times of the body. Ideally, this should cause the neck and the pore body to be filled by condensed vapours at the same pressure. By the time the pressure for neck filling (considering cylindrical meniscus) is attained, the exerted pressure is more than sufficient to fill the pore body (considering hemispherical meniscus) with condensed vapours (Horvath, G. and Kawazoe, 1983). The authors applied the Kelvin Equation (2.0) to the following diagrammatic model as illustrated in Figure 1.0 (Horvath, and Kawazoe, 1983). The radius (r_p) in the ideal and simplified

Corresponding author: Nuradeen, T. ✉ nuradeen.tanko@bazeuniversity.edu.ng ✉ Department of Petroleum and Gas Engineering, Baze University, Abuja, FCT, Nigeria.

JOURNAL OF SCIENCE TECHNOLOGY AND EDUCATION 9(3), SEPTEMBER, 2021
ISSN: 2277-0011; Journal homepage: www.atbuftejoste.com

situation of strict thermodynamic reversibility will be expected to have a vertical riser effect of pore filling according to the above derived Kelvin Equation (2.0).

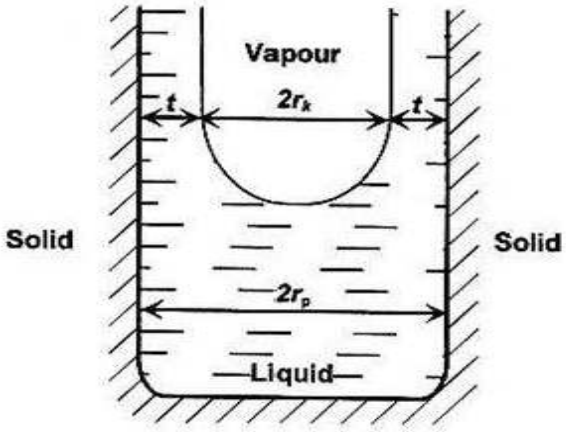

Figure 1.0: The relationship between Kelvin radius and the pore radius (r_p) in a cylindrical mesopore

Furthermore, the work of Rouquerol et al. (1999) reports that the Kelvin Equation (2.0) probably underestimates pore size and that its reliability may not extend below a pore size of ~ 7.5 nm. For a cylindrical pore shape, it seems reasonable to assume that the condensate has a meniscus of hemispherical form and radius (r_k), however as some physisorption has already occurred on the mesopore walls, it is evident that (r_p) and (r_k) is not equal, as defined in Figure 1.0. If the thickness of the adsorbed multilayer is t and has a finite contact angle, θ, which is assumed to be zero, the radius of the cylindrical pore can be written as:

$$r_p = r_k \cos\theta + t = r_k + t \qquad (3.0)$$

Nevertheless, the BJH method is undoubtedly the most widely accepted method for the analysis of nitrogen adsorption/desorption PSD (Rouquerol et al., 2007), and thus, it has been adopted in this study.

In this paper, a novel multi-technique experimental approach will be used to derive structural-topological relationships to understand the mechanism of ultimate entrapment in porous materials. Aforementioned, several researchers used two and three-dimensional bond networks simulation to determine the relationships between structural and transport properties in artificial porous materials. Other workers used the basic Corrugated Pore Structure Model (CPSM). Both analytical and basic experimental and simulation have shown an increase in Mercury entrapment as the variance of the PSD gets wider. In this regard, this paper will explore this simulation correlation on a range of porous alumina and silica pellets of spherical or cylindrical geometries.

MATERIALS AND METHODS

The materials studied in this work are commercially available, chemically pure mesoporous silica and alumina catalyst support pellets with simplified pore sizes, pore size distribution, and surface chemistry. As highlighted in Table 1.0, the materials have a pore size in the range of 7-30 nm. The majority of the materials have a unimodal structure except for one bimodal structured material (AL3984T).

Table 1.0: A range of alumina and Silica materials tested

S/N	Sample	Material	Pellet form	Voidage	Nominal diameter (mm)
1	Aerosil	Silica (SiO_2)	Fumed sphere	N/D[a*]	3.5
2	AL3984T	Alumina (Al_2O_3)	Tablet	0.59	3.0

Corresponding author: Nuradeen, T. ✉ *nuradeen.tanko@bazeuniversity.edu.ng* ✉ *Department of Petroleum and Gas Engineering, Baze University, Abuja, FCT, Nigeria.*

S/N	Sample	Material	Pellet form	Voidage	Nominal diameter (mm)
3	AL3992E	Alumina (Al_2O_3)	Extrudate	0.65	3.0
4	C10	Silica (SiO_2)	Gel sphere	0.66	3.0
5	C30	Silica (SiO_2)	Gel sphere	0.69	3.0
6	P7129	Silica (SiO_2)	Gel sphere	0.67	3.0
7	Q17/6	Silica (SiO_2)	Gel sphere	0.49	3.5
8	S980A	Silica (SiO_2)	Gel sphere	0.6	3.0
9	S980G	Silica (SiO_2)	Gel sphere	0.61	2.2
10	Silica Alumina	Silica and Alumina (Al_2O_5Si)	Extrudate	0.60	0.5

Note: a* – Not detected

EXPERIMENTAL CONSIDERATION

Nitrogen Sorption

On each sample, a nitrogen sorption experiment was carried out at 77K using a Micromeritics accelerated surface area porosimeter (ASAP) 2010 apparatus and AutoPore III 9420 mercury porosimeter were used. The AutoPore III 9420 mercury porosimeter is designed to perform a low-pressure analysis of four samples at one time. The equipment is designed to perform two high-pressure analyses at the same time. The equipment measures the intruded volume about the mass of the sample at a specific pressure; this pressure can be converted to an equivalent Laplace diameter according to the Washburn equation $\left[\Delta P = \frac{2\gamma_{HG}\cos\theta}{r_p}\right]$. The amount of mercury intruded is determined by the fall in the level of the interface between the mercury and the compressing fluid. A value of 0.485 Nm^{-1} at 25 ˚C is generally accepted for surface tension and a fixed value of 130° for the contact angle, as a result, were adopted in this study. If less than four samples are to be analysed, a blank rod must be installed in the unused low-pressure ports. Vacuum conditions cannot be achieved if penetrometers or blank rods are not installed in an unused pressure port.

Porous materials are prone to adsorb water or other chemicals, and therefore the sample has to be cleared of these contaminants before the analysis by heating. The purpose of the thermal pre-treatment for each sample was to drive any physisorbed water on the sample leaving the morphology of the sample itself unchanged. A pre-treatment condition of 250 °C for 4 hours used by Rigby et al. (2008) was adopted for this study. A powder penetrometer (3cc powder) was used due to the small physical size of the materials. The weight of the empty sample flask was registered before introducing the sample. The sample (~0.7 g) was loaded into the penetrometer, which consisted of a sample cup connected to a metal-clad, precision-bore, and glass capillary stem. A vacuum-tight seal (Apiezon H) was used to fill the inevitable roughness of the ground glass lip and polished surface. Care was taken when applying the grease as too much grease exposes the sample to an unwanted coating, whilst too little grease results in an imperfect seal.

The penetrometers were sealed with spacers over the stem and placed in low-pressure ports, where the sample was evacuated to remove air and moisture. The sample cell was evacuated and filled with mercury while the entire system was still under reduced pressure. The first data point was taken at a pressure of 3000 to 4000 Pa or higher. At the end of the low-pressure analysis, the weight of the penetrometer filled with mercury and sample was determined. The measured value determines the bulk density of the sample by using corresponding blank runs as a reference. Once the pre-weighed sample from the low-pressure analyses port was transferred to the high-pressure system, the sample and the injected mercury from the low-pressure system was surrounded by hydraulic fluid and pressurised up to 414 MPa. Both chambers were tightly closed and had sufficient high-pressure fluid drawn into the vent valve. If the fluid was above the visible ledge level, excess fresh fluid was removed to bring the level to the ledge.

To calculate the true volume intrusion of mercury into the pores of a sample, a correction

Corresponding author: Nuradeen, T. ✉ nuradeen.tanko@bazeuniversity.edu.ng ✉ Department of Petroleum and Gas Engineering, Baze University, Abuja, FCT, Nigeria.

was made to account for the compression of mercury, sample cell and sample. Compressibility (β^0) is the fractional change in volume per unit pressure change and therefore a major effect that has to be addressed (Orr, 1969). Ideally, this problem can be corrected by a corresponding blank run using a non-porous sample of the same material. However, the blank run does not always solve the problem as encountered in the course of these experiments. One of the adjustments made was to create separate blank runs with the same respective equilibration time as those used in the experiments.

Furthermore, on each sample, a nitrogen sorption experiment was carried out at 77K using a Micromeritics accelerated surface area porosimeter (ASAP) 2010 apparatus. Initially, about 0.2 g of the sample was left under vacuum for 4 hours at a pressure of 0.27 Pa as recommended by Rigby et al. (2008). The purpose of the thermal pre-treatment for each sample was to drive any physisorbed water on the sample while leaving the morphology of the sample itself unchanged. The sample tube and its contents were then re-weighed after cooling to room temperature. Thus, the dry weight of the sample before being transferred to the analysis port for the automated analysis procedure was measured. A full adsorption/desorption micro/mesoporous was carried out since the samples' characteristics were unknown. The calculation of the dead volume of the flask (free space analysis) was carried out by using helium. The dead space was the volume of the sample tube excluding the sample itself. As also recommended by Rigby et al. (2008), the equilibration time for the diffusion of nitrogen molecules to access most of the pores present in these materials was set at forty-five seconds. In the Kelvin equation $\left[RT \ \ln \ x = \frac{-2\gamma_{LV} V_L \cos \theta}{r_k} \right]$, the adsorbate property factor was taken as 9.53×10^{-10} m.

Furthermore, it was assumed that the fraction of pores open at both ends was zero, for both adsorption and desorption. Thus, capillary condensation commenced at the closed end of a pore to form a hemispherical meniscus, and the process of evaporation commenced at a hemispherical meniscus.

For the determination of Pore Surface Area, the Branauer Emmet Teller (BET) equation derived by Brunauer et al. (1938) for multilayer adsorption is given by:

$$\frac{P}{V(P_0 - P)} = \frac{1}{cV_m} + \frac{c-1}{cV_m}\frac{P}{P_0} \quad (4.0)$$

A plot $\frac{P}{V(P_0 - P)}$ against $\frac{P}{P_0}$ yields a line of slope $\frac{c-1}{cV_m}$ and intercept $\frac{1}{cV_m}$. The BET Equation (4.0) holds for Type I, Type II, Type III and Type IV isotherms, depending on the nature of the constant c (Schreiber et al., 2006). The BET surface area (a_{BET}) can be evaluated from monolayer capacity by using Equation 5.0.

$$(a_{BET}) = V_m \sigma_a N_A \quad (5.0)$$

The value σ_a used for nitrogen is based on an assumption that the nitrogen molecules are spherical and rest on a plane surface with a packing similar to that in the bulk liquid.

Mercury Porosimetry (MP)

On each sample, a nitrogen sorption experiment was carried out. The AutoPore III 9420 mercury porosimeter is designed to perform a low-pressure analysis of four samples at one time. The equipment is designed to perform two high-pressure analyses at the same time. The equipment measures the intruded volume about the mass of the sample at a specific pressure; this pressure can be converted to an equivalent Laplace diameter according to the Washburn equation $\left[\Delta P = \frac{2\gamma_{HG} \cos \theta}{r_p} \right]$.

The amount of mercury intruded is determined by the fall in the level of the interface between the mercury and the compressing fluid. A value of 0.485 Nm^{-1} at 25 ˚C is generally accepted for surface tension and a fixed value of 130° for the contact angle, as a result, were adopted in this study. If less than four samples are to be analysed, a blank rod must be installed in the unused low-pressure ports. Vacuum conditions can not be achieved if penetrometers or blank rods are not installed in an unused pressure port.

Porous materials are prone to adsorb water or other chemicals, and therefore the sample has to be cleared of these contaminants before the analysis by heating. The purpose of the thermal pre-treatment for each sample was to drive any physisorbed water on the sample leaving the morphology of the sample itself unchanged. A

Corresponding author: Nuradeen, T. ✉ nuradeen.tanko@bazeuniversity.edu.ng ✉ Department of Petroleum and Gas Engineering, Baze University, Abuja, FCT, Nigeria.

pre-treatment condition of 250 °C for 4 hours used by Rigby et al. (2008) was adopted for this study. A powder penetrometer (3cc powder) was used due to the small physical size of the materials. The weight of the empty sample flask was registered before introducing the sample. The sample (~ 0.7 g) was loaded into the penetrometer, which consisted of a sample cup connected to a metal-clad, precision-bore, and glass capillary stem. A vacuum-tight seal (Apiezon H) was used to fill the inevitable roughness of the ground glass lip and polished surface. Care was taken when applying the grease as too much grease exposes the sample to an unwanted coating, whilst too little grease results in an imperfect seal.

The penetrometers were sealed with spacers over the stem and placed in low-pressure ports, where the sample was evacuated to remove air and moisture. The sample cell was evacuated and filled with mercury while the entire system was still under reduced pressure. The first data point was taken at a pressure of 3000 to 4000 Pa or higher. At the end of the low-pressure analysis, the weight of the penetrometer filled with mercury and sample was determined. The measured value determines the bulk density of the sample by using corresponding blank runs as a reference. Once the pre-weighed sample from the low-pressure analyses port was transferred to the high-pressure system, the sample and the injected mercury from the low-pressure system was surrounded by hydraulic fluid and pressurised up to 414 MPa. Both chambers were tightly closed and had sufficient high-pressure fluid drawn into the vent valve. If the fluid was above the visible ledge level, excess fresh fluid was removed to bring the level to the ledge. To calculate the true volume intrusion of mercury into the pores of a sample, a correction was made to account for the compression of mercury, sample cell and sample. Compressibility (β^0) is the fractional change in volume per unit pressure change and therefore a major effect that has to be addressed (Orr, 1969). Ideally, this problem can be corrected by a corresponding blank run using a non-porous sample of the same material. However, the blank run does not always solve the problem as encountered in the course of these experiments. One of the adjustments made was to create separate blank runs with the same respective equilibration time as those used in the experiments.

RESULTS AND DISCUSSION

During MPE, batch variability was addressed, and thus, to allow for the variation of support structure between pellets of the same batch and to test the reproducibility of measurements, replicate measurements were made for all samples. The reported parameters in this section are the mean of these sets used. After each pressure change, the volume of mercury within the sample was then allowed to come to equilibrium over a while. The equilibration time at each of the increasing applied pressures of mercury was set at 50 s.

An estimate of the total mercury trapped following depressurization was found from the mercury retraction curve. The entrapped mercury is the difference between the volume at the end of the retraction curve and the corresponding pressure point on the intrusion curve (separating interparticle and intraparticle intrusion). Also, the volume of entrapped mercury determines the level of remaining open porosity. The porosity is obtained by taking the ratio of the pore volume and the total volume. It is noteworthy to mention that AutoPore III 9420 mercury porosimeter calculates the solution directly from the raw data.

Furthermore, during Nitrogen Sorption experiments, batch variability was addressed, and thus, to allow for the variation of support structure between pellets from the same batch and to test the reproducibility of measurements, replicate measurements are used. The reported parameters in this section are the mean of these sets used. Moreover, during experiments, the relative pressure was either increased or decreased in small steps, and a small volume of nitrogen, either enters or leaves, the sample.

The BET surface area $\left(a_{BET}\right)$ was evaluated from the monolayer capacity. The following pressure range, $0.1 < x \leq 0.3$, was used for the BET plots. For each data set, the BET plots yielded a coefficient of determination with linear regression $\left(R^2\right)$ greater than 0.999. An incorrect nitrogen molecular area can result in an error in the estimation of the surface area, and thus, the molecular area of the adsorbate molecule in the completed monolayer, σ_a, was assumed to be 0.162 nm^2.

Tables 2.0 presents the estimated Mercury entrapment, Absolute Porosity, Pore

Corresponding author: Nuradeen, T. ✉ nuradeen.tanko@bazeuniversity.edu.ng ✉ Department of Petroleum and Gas Engineering, Baze University, Abuja, FCT, Nigeria.

diameter, BET surface area, and variance of Pore Size Distribution of the investigated materials. The reported uncertainties indicate the spread of the results over samples from the same batch and the error associated with the technique. It is noteworthy to mention that the result obtained showed strong interactions between the adsorbate and adsorbents $(c > 100)$. Figure 2.0 presents the effect of PSD on Mercury entrapment. It can be seen from Figure 2.0 that the amount of ultimate entrapment increased with an increase in the variance of the PSD.

Table 2.0: Average key pore geometry characteristics obtained by various methods. The error quoted is the standard

Sample	Characterization Technique			
	Mercury Porosimetry		Gas Porosimetry	
	Porosity	Entrapment	BET Surface area	The variance of PSD (σ/μ)
	(%)	(%)	(m^2/g)	(-)
Aerosil	66.99 ± N/A	13.66 ± N/A	162.00 ± 24.00	0.900 ± 0.23
AL3984T	56.50 ± 1.85	15.51 ± 0.80	103.00 ± 9.04	0.722 ± 0.05
AL3992E	66.60 ± 0.82	12.23 ± 2.94	159.00 ± 29.02	0.585 ± 0.04
C10	69.70 ± 3.13	9.46 ± 1.23	326.00 ± 32.56	0.356 ± 0.11
C30	70.51 ± 3.43	3.45 ± 0.23	81.00 ± 4.15	0.190 ± 0.02
P7129	65.54 ± 0.01	50.13 ± 3.04	N/A*	N/A*
Q17/6	48.53 ± 1.73	20.26 ± 5.21	156.00 ± 3.90	0.460 ± 0.09
S980A	72.35 ± 3.95	9.36 ± 0.89	192.00 ± 15.44	0.511 ± 0.16
S980g	72.41 ± 0.26	15.18 ± 0.73	63.00 ± 2.56	0.143 ± N/A
Silica Alumina	60.79 ± 0.35	20.69 ± 2.53	198.00 ± 2.34	1.25 0± 0.50

Note: N/A* – Not Applicable

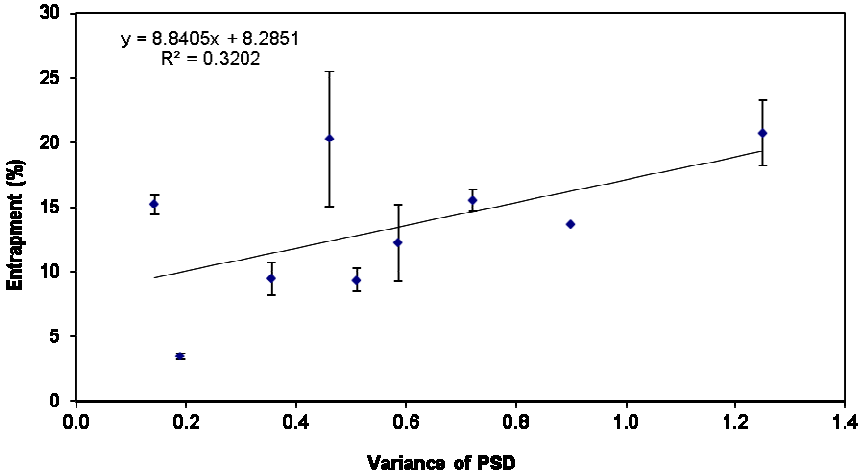

Figure 2.0: Relating the ultimate entrapment with the variance of the PSD

A novel multi-technique approach has been used to derive structural-topological relationships to understand the mechanism of ultimate entrapment in porous materials. As detailed in Section I, several researchers used two and three-dimensional bond networks simulation to

Corresponding author: Nuradeen, T. ✉ *nuradeen.tanko@bazeuniversity.edu.ng* ✉ *Department of Petroleum and Gas Engineering, Baze University, Abuja, FCT, Nigeria.*

determine the relationships between structural and transport properties in artificial porous materials. Other workers used the basic Corrugated Pore Structure Model (CPSM). Both analytical and basic experimental have shown an increase in Mercury entrapment as the variance of the PSD gets wider. In this regard that this section discusses these correlations for structural-topological relationships that were tested with experimental results for a range of porous alumina and silica pellets of spherical or cylindrical geometries.

During the MPE, the pressure was either increased or decreased in small steps, and thus, this might have affected the pore network of the samples. The high hydraulic pressure applied on materials during intrusion can sometimes lead to the partial collapse of the pore network or alteration of the sample during the experiments. Therefore, these pressures may also give rise to the potential collapse of the unoccupied pores. Consequently, this will reduce the number of large pores and give false entrapment values (Gregg and Sing, 1982). This research has been altered to avoid such limitations, such as the mechanical damage of samples. It is noteworthy to mention that all samples were visually observed after the experiments, to ensure that the high hydraulic pressure applied on the materials did not cause elastic or permanent structural changes. The majority of the test samples retained their external structural stability except for C10, AL3992E, and Silica Alumina. Furthermore, the presence of pore shielding in these materials was previously studied by Diamond (2000). It was found that no structural deformation or collapse occurred for these samples.

The mercury entrapment quoted in Table 2.0 was barely affected by the experimental equilibration time, and thus, was considered as the ultimate entrapment. The gas adsorption studies carried out on all samples revealed isotherms of type IV classification with reproducible type H2 hysteresis loops. The PSD of the materials was obtained by using the Barrett et al. (1951) method. The variance of the PSD distribution of the samples is shown in Table 2.0. It can be seen in Figure 1.0 that the amount of ultimate entrapment increased with an increase in the variance of the PSD.

To support this correlation, static analysis was carried out to rule out any possibility of random chance. A common alpha level for research is 0.10 and was thus adopted in this study (Chatfield, 1983). The correlation coefficient obtained for the correlation was 0.566, and the number of data points is nine. Therefore, by using the critical value table for Pearson's correlation coefficient (Chatfield, 1983), it can be concluded that the correlation is statistically significant. This significant finding is in good agreement with the mercury simulation works of (Androutsopoulost & Mann, 1978; Conner et al., 1984; Lapidus, Lane, Ng, & Conner, 1985l Portsmouth, 1990; Tsakiroglou and Payatakes, 1990).

CONCLUSION

A novel multi-technique approach has been used to predict the relationships between PSD and mercury entrapment. A range of porous alumina and silica pellets of spherical or cylindrical geometries were investigated. These samples had strong interactions between the adsorbate and adsorbent, and thus is susceptible to advanced condensation phenomena that will result in a narrow PSD than it exists in reality. In addition, the assumed cylindrical pore shape by the porosimetry techniques ought to affect the structural-topological relationships. Nevertheless, in this study, a good statistical correlation was obtained. Consequently, the effect of advanced condensation and the assumed pore shape did not have any effect on the correlations. It was found that mercury entrapment increases with an increase in the variance of the PSD, despite limitations on the measurement of this descriptor. This finding is in good agreement with several two and three-dimensional bond networks simulation work and basic experimental work on Corrugated Pore Structure Model.

REFERENCES

Abell, A. B., Willis, K. L., & Lange, D. A. (1999). Mercury intrusion porosimetry and image analysis of cement-based materials. *Journal of Colloid and Interface Science*, *211*(1), 39–44. https://doi.org/10.1006/jcis.1998.5986

Allen, T. (1999). *Particle size measurement*. Dordretch, The Netherlands: Kluwer Academic publishers.

Androutsopoulost, G. P., & Mann, R. (1978). Evaluation Using of Mercury a Network Pore Structure Experiments. *Chemical Engineering Science*, *34*, 1203–1212.

Bafarawa, B., Nepryahin, A., Ji, L., Holt, E. M., Wang, J., & Rigby, S. P. (2014). Combining mercury thermoporometry

Corresponding author: Nuradeen, T. ✉ *nuradeen.tanko@bazeuniversity.edu.ng* ✉ *Department of Petroleum and Gas Engineering, Baze University, Abuja, FCT, Nigeria.*

with integrated gas sorption and mercury porosimetry to improve the accuracy of pore-size distributions for disordered solids. *Journal of Colloid and Interface Science*, *426*, 72–79. https://doi.org/10.1016/j.jcis.2014.03.053

Barrett, E. P., Joyner, L. G., & Halenda, P. P. (1951). The Determination of Pore Volume and Area Distributions in Porous Substances. I. Computations from Nitrogen Isotherms. *Journal of the American Chemical Society*, *73*(1), 373–380. https://doi.org/10.1021/ja01145a126

Brunauer, S., Emmett, P. H., & Teller, E. (1938). Adsorption of Gases in Multimolecular Layers. *Journal of the American Chemical Society*, *60*(2), 309–319. https://doi.org/10.1021/ja01269a023

Chatfield, C. (1983)*Statistics for technology: A course in applied statistics*. Chapman & Hall/CRC.

Conner, W. C., Lane, A. M., & Hoffman, A. J. (1984). Measurement of the morphology of high surface area solids: hysteresis in mercury porosimetry. *Journal of Colloid And Interface Science*, *100*(1), 185–193. https://doi.org/10.1016/0021-9797(84)90424-7

Diamond, S. (2000). Mercury porosimetry. An inappropriate method for the measurement of pore size distributions in cement-based materials. *Cement and Concrete Research*, *30*(10), 1517–1525. https://doi.org/10.1016/S0008-8846(00)00370-7

Drewry, H. P. G., & Seaton, N. A. (1995). Continuum random walk simulations of diffusion and reaction in catalyst particles. *AIChE Journal*, *41*(4), 880–893. https://doi.org/10.1002/aic.690410415

Ghaly, G., Beurroies, I., & Ragai, J. (2009). Mesoporous titania gels prepared from titanous chloride and ammonia: SEM, nitrogen adsorption, thermoporometry and mercury porosimetry studies. *Adsorption Science and Technology*, *27*(10), 937–945. https://doi.org/10.1260/0263-6174.27.10.937

Giesche, H. (2006). Mercury porosimetry: A general (practical) overview. *Particle and Particle Systems Characterization*, *23*(1), 9–19. https://doi.org/10.1002/ppsc.200601009

Hitchcock, I., Malik, S., Holt, E. M., Fletcher, R. S., & Rigby, S. P. (2014). Impact of chemical heterogeneity on the accuracy of pore size distributions in disordered solids. *Journal of Physical Chemistry C*, *118*(35), 20627–20638. https://doi.org/10.1021/jp505482p

Horvath, G. and Kawazoe, K. (1983). Method for calculation effective pore size distribution in molecular sieve carbon. *J. Chem. Eng. Japan*, *16*(12), 470–475.

Ioannidis, M. A., & Chatzis, I. (1993). Network Modelling of Fore Structure and. *Engineering*, *48*(5), 951–972.

Lapidus, G. R., Lane, A. M., Ng, K. M., & Conner, W. C. (1985). Interpretation of Mercury Porosimetry Data Using a Pore-Throat Network Model. *Chemical Engineering Communications*, *38*(1–2), 33–56. https://doi.org/10.1080/00986448508911294

Lastoskie, C., Gubbins, K. E., & Quirke, N. (1993). Pore size distribution analysis of microporous carbons: A density functional theory approach. *Journal of Physical Chemistry*, *97*(18), 4786–4796. https://doi.org/10.1021/j100120a035

Liu, H., & Seaton, N. A. (1994). Determination of the connectivity of porous solids from nitrogen sorption measurements-III. Solids containing large mesopores. *Chemical Engineering Science*, *49*(11), 1869–1878. https://doi.org/10.1016/0009-2509(94)80071-5

Lowell, S., & Shields, J. E. (1981). Hysteresis, entrapment, and wetting angle in mercury porosimetry. *Journal of Colloid And Interface Science*, *83*(1), 273–278. https://doi.org/10.1016/0021-9797(81)90032-1

Ma, H. (2014). Mercury intrusion porosimetry in concrete technology: Tips in measurement, pore structure parameter acquisition and application. *Journal of Porous Materials*, *21*(2), 207–215. https://doi.org/10.1007/s10934-013-9765-4

Meyer, H. I. (1953). Pore distribution in porous media. *Journal of Applied Physics*, *24*(5), 510–512. https://doi.org/10.1063/1.1721319

Moro, F., & Böhni, H. (2002). Ink-bottle effect in

Corresponding author: Nuradeen, T. ✉ *nuradeen.tanko@bazeuniversity.edu.ng* ✉ *Department of Petroleum and Gas Engineering, Baze University, Abuja, FCT, Nigeria.*

mercury intrusion porosimetry of cement-based materials. *Journal of Colloid and Interface Science*, *246*(1), 135–149. https://doi.org/10.1006/jcis.2001.7962

Nguyen, P. T. M., Do, D. D., & Nicholson, D. (2011). On the hysteresis loop of argon adsorption in cylindrical pores. *Journal of Physical Chemistry C*, *115*(11), 4706–4720. https://doi.org/10.1021/jp111254j

Orr, C. (1969). Application of mercury penetration to materials analysis. *Powder Technology*, *3*(1), 117–123. https://doi.org/10.1016/0032-5910(69)80064-1

Pirard R., Heinrichs B., Pirard J.P. in: McEnaney B., Mays T.J., Rouquerol J., Reinoso R.F., Sing

K.S.W., Unger (Eds.) K.K. (1997). *Characterisation of Porous Solids IV, Royal Society of Chemistry*. Cambridge.

Portsmouth, R.L., and Gladden, L.F. (1991). Mercury porosimetry as a probe of pore connectivity. *Chemical Engineering Research and Design*, 70 (1), 63-70

Portsmouth, R.L., and Gladden, L.F. (1992). Mercury porosimetry as a probe of pore connectivity. *Chemical Engineering Research and Design*, 1992, 70 (1), 63-70.

Rasmussen, C. J., Gor, G. Y., & Neimark, A. V. (2012). Monte Carlo simulation of cavitation in pores with nonwetting defects. *Langmuir*, *28*(10), 4702–4711. https://doi.org/10.1021/la300078k

Rigby, S. P. (2000). A hierarchical structural model for the interpretation of mercury porosimetry and nitrogen sorption. *Journal of Colloid and Interface Science*, *224*(2), 382–396. https://doi.org/10.1006/jcis.1999.6707

Rigby, S. P., & Chigada, P. I. (2009). Interpretation of integrated gas sorption and mercury porosimetry studies of adsorption in disordered networks using mean-field DFT. *Adsorption*, *15*(1), 31–41. https://doi.org/10.1007/s10450-008-9147-4

Rigby, S. P., Chigada, P. I., Evbuomvan, I. O., Chudek, J. A., Miri, T., Wood, J., & Bakalis, S. (2008). Experimental and modelling studies of the kinetics of mercury retraction from highly confined geometries during porosimetry in the transport and the quasi-equilibrium regimes. *Chemical Engineering Science*, *63*(24), 5771–5788. https://doi.org/10.1016/j.ces.2008.08.027

Rigby, S. P., Chigada, P. I., Wang, J., Wilkinson, S. K., Bateman, H., Al-Duri, B., … Miri, T. (2011). Improving the interpretation of mercury porosimetry data using computerised X-ray tomography and mean-field DFT. *Chemical Engineering Science*, *66*(11), 2328–2339. https://doi.org/10.1016/j.ces.2011.02.031

Rigby, S. P., Fletcher, R. S., & Riley, S. N. (2003). Determination of the cause of mercury entrapment during porosimetry experiments on sol-gel silica catalyst supports. *Applied Catalysis A: General*, *247*(1), 27–39. https://doi.org/10.1016/S0926-860X(03)00059-0

Rouquerol, J., Llewellyn, P., & Rouquerol, F. (2007). Is the BET equation applicable to microporous adsorbents? *Studies in Surface Science and Catalysis*, *160*, 49–56. https://doi.org/10.1016/s0167-2991(07)80008-5

Schreiber, J., Bell, F., Grüner, F., Schramm, U., Geissler, M., Schnürer, M., … Habs, D. (2006). Analytical model for ion acceleration by high-intensity laser pulses. *Physical Review Letters*, *97*(4), 1–4. https://doi.org/10.1103/PhysRevLett.97.045005

Seaton, N. A., Walton, J. P. R. B., & quirke, N. (1989). A new analysis method for the determination of the pore size distribution of porous carbons from nitrogen adsorption measurements. *Carbon*, *27*(6), 853–861. https://doi.org/10.1016/0008-6223(89)90035-3

Stefan, D., Harald, B., Anna, S., Günter, K., Thomas, R. (2006). Determination of Porosity and Pore. Connectivity in Fieldspares from Soils of Granite and Saprolite. Soil Science: 171(9), 675-694

Tsakiroglou, C.D., and Payatakes, A.C. (1990). A new simulator of mercury porosimetry for the characterization of porous materials. *Journal of Colloid and Interface Science*, 137, 315-339

Corresponding author: Nuradeen, T. ✉ nuradeen.tanko@bazeuniversity.edu.ng ✉ Department of Petroleum and Gas Engineering, Baze University, Abuja, FCT, Nigeria.

Wardlaw, N. C., & McKellar, M. (1981). Mercury porosimetry and the interpretation of pore geometry in sedimentary rocks and artificial models. *Powder Technology*, *29*(1), 127–143. https://doi.org/10.1016/0032-5910(81)85011-5

Washburn, E. W. (1921). The dynamics of capillary flow. Phys. Rev., 1921, 17, 273-283

Corresponding author: Nuradeen, T. ✉ *nuradeen.tanko@bazeuniversity.edu.ng* ✉ *Department of Petroleum and Gas Engineering, Baze University, Abuja, FCT, Nigeria.*